Transactions of the Materials Research Society of Japan 28 [3] 911-914 (2003)

Band Structure Calculation of TTTA Crystal

Miou Furuya[1], Kaoru Ohno[1], Tsuguo Morisato[2], Yoshiyuki Kawazoe[2] and Jun Takeda[1]

[1]Graduate School of Engineering, Yokohama National University, 79-5 Tokiwadai, Hodogaya-ku, Yokohama 240-8501, Japan
Fax: 81-45-339-4254, e-mail: d02gd227@ynu.ac.jp, ohno@ynu.ac.jp, jun@ynu.ac.jp

[2]Institute for Materials Research, Tohoku University, 2-1-1 Katahira, Aoba-ku, Sendai 980-8577
Fax: 81-22-215-2052, e-mail: morisato@imr.edu, kawazoe@imr.edu

TTTA (1,3,5-trithia-2,4,6-triazapentalenyl) molecular crystal which was recently found by Fujita and Awaga undergoes a first-order phase transition between a paramagnetic high-temperature (HT) phase and a diamagnetic low-temperature (LT) phase and exhibits magnetic bistability. In this paper, the electronic structure including magnetic and optical properties of the TTTA crystal is investigated theoretically by means of the all-electron mixed basis approach in the local density approximation (LDA) of density functional theory. The Fermi level exists in the HT phase which has a uniform one-dimensional stacking of the molecules, while 0.8 eV band gap exists in the LT phase in which dimerization of the molecules occurs in the stacking direction. This explains the paramagnetism and the diamagnetism in the HT and LT phases, respectively. The dielectric response function as well as the reflection spectrum are calculated within the random phase approximation (RPA) on the same approach and compared with the experimental data.

Key words: molecular crystal, *ab initio* method, band structure, dielectric response function, and reflection spectrum

1. INTRODUCTION

Magnetic and optical properties of molecule-based materials have been studied extensively. In particular, crystals composed of organic radical molecules have attracted great attention due to their potential in future molecular magnetic and optical devices. They are also expected to play a major role in novel materials research. An organic radical, TTTA (1,3,5-trithia-2,4,6-triazapentalenyl), is a good example of such materials.

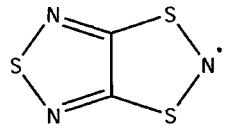

Fig. 1 Structure of TTTA molecule.

As shown in Fig. 1, TTTA consists of three sulfur, three nitrogen and two carbon atoms. It has a flat heterocyclic triazyl structure. Fujita and Awaga [1] found that the TTTA crystal exhibits a first-order phase transition between a paramagnetic high-temperature (HT) phase and a diamagnetic low-temperature (LT) phase, with a surprisingly wide thermal hysterisis loop over near the room temperature. They also determined the crystal structures for the both phases by means of the X-ray diffraction experiment [1,2]. Recently Takeda *et al.* found also experimentally that a photo-induced magnetic phase transition takes place in this system and its magnetic properties can be optically controlled [3].

In the present paper, we carry out the structural optimization and the electronic structure calculations for the both phases of TTTA crystal and derive the magnetic and optical properties from the resulting band structures. In particular, we discuss the existence of the band gap and calculate the reflection spectrum as well as the dielectric response function. For all these calculations, we adopt the *ab initio* methods within the local density approximation (LDA) in density functional theory.

2. CRYSTAL STRUCTURES

In order to check the crystallography data determined experimentally [1,2], we first carried out the structural optimization for the both phases of the TTTA crystal in the following way. Assuming the crystal symmetries (the HT phase belongs to the monoclinic $P2_1/c$ and the LT phase belongs to the triclinic $P\bar{1}$), lattice constants and angles of the unit cell given by the X-ray diffraction measurement [1], we optimized all atomic positions inside the unit cell by means of the standard *ab initio* ultrasoft-pseudopotential approach (VASP) [4] with the 26 Ry cutoff energy for the plane waves (PW's). From this calculation, we confirmed that the position data determined experimentally [2] are reproduced within the error of 0.09 Å. The resulting structures are shown in Figs. 2 and 3, respectively, for the HT and LT phases. The estimated total energy difference between the two phases is 0.31 eV.

Here we briefly summarize the characteristics of the crystal structures for the HT and LT phases. There is a crucial difference in molecular packing in the two phases: The unit cell of the HT phase includes two molecular-plane orientations (Fig. 2), whereas the molecular planes are all parallel in the LT phase (Fig. 3). In addition, in the HT phase, uniform one-dimensional stacking of the radical molecules appears, while, in the LT phase, strong dimerization along the stacking direction appears.

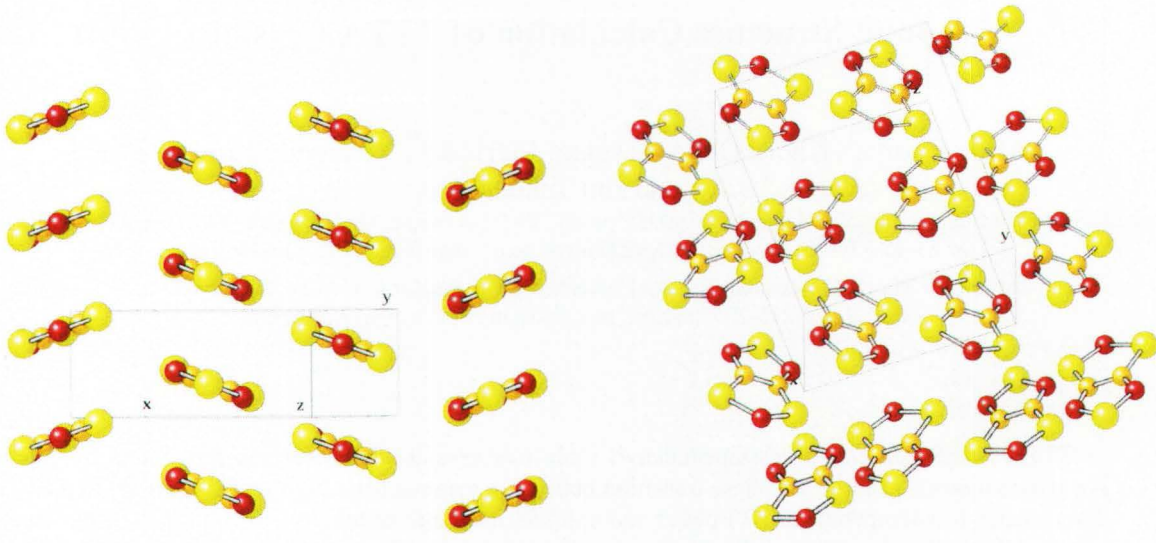

Fig. 2 Side and diagonal views of the columnar structure in the HT phase whose crystal structure is monoclinic. Yellow, red and orange spheres represent sulfur, nitrogen, and carbon atoms, respectively.

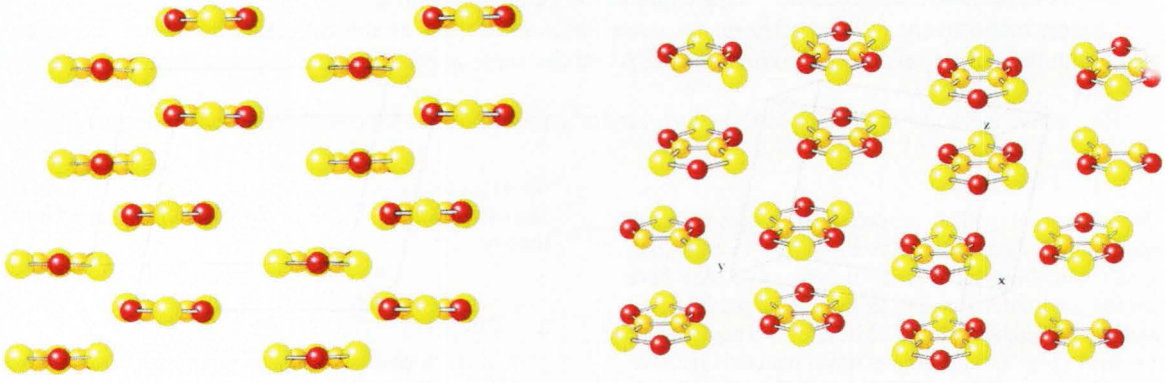

Fig. 3 Side and diagonal views of the columnar structure in the LT phase whose crystal structure is triclinic.

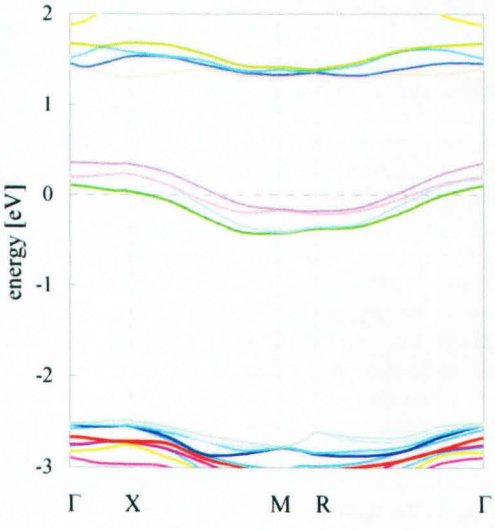

Fig. 4 Band structure of the HT phase. Energy zero is set at the Fermi level.

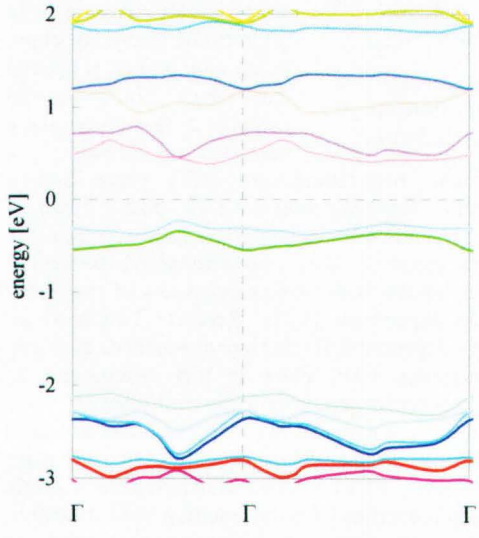

Fig. 5 Band structure of the LT phase. Energy zero is set in the middle of the band gap.

3. ELECTRONIC STRUCTURES

For the elctronic structure calculations, we used the all-electron mixed basis approach [5-7] using both PW's and atomic orbitals (AO's) as a basis set. Here all the core and valence AO's are determined numerically within the non-overlapping atomic spheres by a standard atomic program in Herman-Skillman's framework with the logarithmic radial mesh. For the LDA exchange-correlation functional, we adopt the Ceperley-Alder fitting form [8]. For the present system, we use 208 numerical AO's and 2135 (in the HT phase) or 2401 (in the LT phase) PW's corresponding to a 12 Ry cutoff energy using 36 special k points.

The resulting band structures are shown in Figs. 4 and 5, respectively, for the HT and LT phases. Fermi level exists in the HT phase (Fig. 4). In the LT phase (Fig. 5), because of the dimerization of TTTA molecules, all two-fold degenerate levels split into two separate levels and 0.8eV band gap appears. This clear distinction of the band diagrams must be the origin of Pauli's spin paramagnetism (for a metal) in the HT phase and the closed-shell diamagnetism (for an insulator) in the LT phase.

In view of Figs. 2 and 3, one can recognize that the structural phase transition between the $P2_1/c$ (in the HT phase) and $P\bar{1}$ (in the LT phase) symmetries takes place due to the Jahn-Teller effect, because the static Jahn-Teller effect occurs when the highest occupied level is degenerate and occupied partially by electrons. In such cases, the crystal is distorted spontaneously in order to gain the energy by removing the degeneracy. In the present case, this lattice distortion is characterized by the dimerization of molecules and the corresponding phase transition can be regarded as a kind of Peierls transition (due to the quasi-one-dimensional response of the three-dimensional electronic system) between the HT phase having the uniform one-dimensional stacking and the dimerized LT phase. This explanation is the analogy of the well-known 1D organic radical conductor, TTF-TCNQ [9]. In general, the Peierls instability in 1D electron systems is induced by the electron-phonon interaction, which can develop due to the characteristic topology of the Fermi surface (FS) with a perfect nesting. A 1D metal is unstable towards static periodic lattice distortions below the Peierls temperature because of the nesting property of the FS. Such a distortion opens an energy gap at the new zone boundary, and thus the total energy decreases.

In the present LDA picture, we found the Fermi level in the band structure of the HT phase. This phase is, however, not optically a metal in experiments. How should we consider this discrepancy? The strong electron-electron Coulomb repulsion and the existence of the partially filled bands near the Fermi level could induce a Mott-Hubbard metal-insulator transition, i.e., the transition between a paramagnetic metal and a paramagnetic insulator. We could estimate the on-site Coulomb energy of the HT phase to be about 8 eV, whereas bandwidth is not more than 1eV. We found by carrying out a calculation based on the local spin density approximation (LSDA) instead of the LDA that the four levels around Fermi level break up into two full-filling majority spin levels and two empty minority spin levels, resulting in the spin polarization. This suggests that the instability of the present LDA ground state may occur by the perturbation due to the electron correlation.

4. DIELECTRIC RESPONSE

The frequency and wave-number dependent dielectric response function is given within the random phase approximation (RPA) as [10]

$$\varepsilon(q,\omega)=1+4\pi\chi(q,\omega)$$

$$\chi(q,\omega)=-\frac{2}{\Omega q^2}\sum_k\sum_\lambda\sum_\nu\left[f_0(\varepsilon_{k+q,\lambda})-f_0(\varepsilon_{k,\nu})\right]\times\frac{\left|\langle k+q,\lambda|e^{iq\cdot r}|k,\nu\rangle\right|^2}{\varepsilon_{k+q,\lambda}-\varepsilon_{k,\nu}-\omega-i\delta},$$

where the summations with respect to the level indices λ and ν run over all levels, $\boldsymbol{k}$ is the wave vector inside the first Brillouin zone and $f_0(\varepsilon)$ denotes the Fermi-Dirac distribution function. The factor of 2 in the prefactor is due to the spin multiplicity. There are components which couple transverse and longitudinal electromagnetic disturbances. Using the commutation relation between H and $\boldsymbol{r}$, one may rewrite in the limit $\boldsymbol{q}\rightarrow 0$ as

$$\chi_{\alpha\beta}(0,\omega)=-\frac{2}{3\Omega}\sum_k\sum_\lambda\sum_\nu\frac{\left[f_0(\varepsilon_{k,\lambda})-f_0(\varepsilon_{k,\nu})\right]}{\left(\varepsilon_{k,\lambda}-\varepsilon_{k,\nu}\right)^2}\times\frac{\langle k,\lambda|\nabla_\alpha|k,\nu\rangle\cdot\langle k,\nu|\nabla_\beta|k,\lambda\rangle}{\varepsilon_{k,\lambda}-\varepsilon_{k,\nu}-\omega-i\delta},$$

where the indices α and β of $\chi_{\alpha\beta}$ represent the directions x, y, z of the induced and external electric fields. In what follows we will consider the LT phase only. For the present system, we calculate up to 300 levels. The obtained dielectric response function is presented in Figs. 6 and 7 with the electric field $\boldsymbol{E}$ of lights parallel and perpendicular to the stacking axis, respectively. There is a significant difference between Figs. 6 and 7, which indicates the dielectric response depends strongly on the direction of the electric field. We confirmed that their real and imaginary parts satisfy the Kramers-Kronig relation with high accuracy.

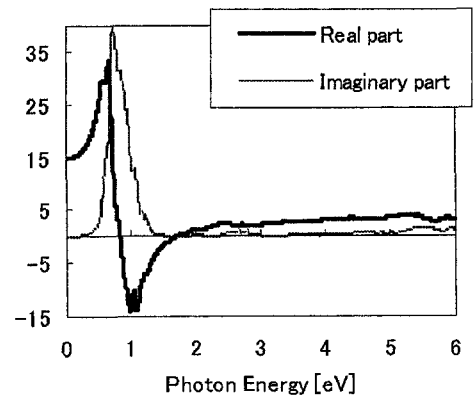

Fig.6 Dielectric response function for the electric field perpendicular to the stacking direction in the LT phase. The thick and thin curves represent, respectively, the real part $\varepsilon_1(\omega)$ and the imaginary part $\varepsilon_2(\omega)$.

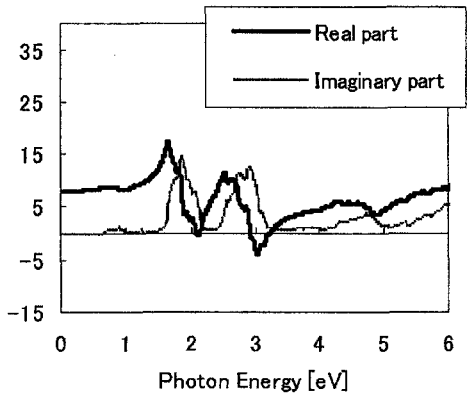

Fig.7 Dielectric response function for the electric field parallel to the stacking direction in the LT phase. The thick and thin curves represent, respectively, the real part $\varepsilon_1(\omega)$ and the imaginary part $\varepsilon_2(\omega)$.

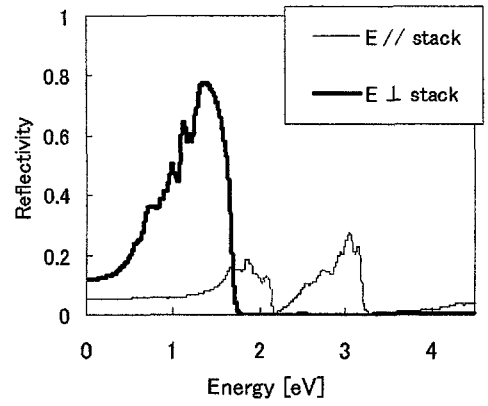

Fig. 8 Reflectivity spectrum in the LT phase. The thick and thin curves represent the results with the electric field ***E*** of the lights parallel and perpendicular to the stacking axis, respectively.

Figure 8 represents the reflectivity spectrum in the LT phase. The thick and thin curves represent the reflectivities for the electric field ***E*** of lights parallel and perpendicular to the stacking axis, respectively. If we compare these results with the experimental reflection data [2], we find close similarity in the overall behavior, although there is difference in peak positions and amplitudes: The large peak at 1.3 eV in the thick curve (***E*** ⊥ stacking direction) corresponds to the experimental peak at 2.2 eV, while the two peaks at 1.8 eV and at 3.1 eV in the thin curve (***E*** // stacking direction) corresponds to the experimental peaks at 1.9 eV and at 3.4 eV. The amplitude of the calculated reflectivity is overestimated about two or three times larger than the experimental reflectivity. These discrepancies remain to be solved in the future, although a possible explanation on this problem might be as follows: In general, the LDA underestimates the band gap in insulators typically 30-50 %, and this could explain the shift of the peaks. Since the present TTTA molecular crystal is classified undoubtedly into one of the highly correlated systems such as the Mott insulators, the many body effect due to the electron-electron interaction must be inevitably taken into account.

ACKNOWLEDGEMENTS

The authors acknowledge the support of the HITAC SR8000 supercomputing facilities that are owned by the Computer Science Group at the Institute for Materials Research, Tohoku University. The authors also would like to thank Prof. Awaga for helpful discussions.

REFERENCES

[1] W. Fujita and K. Awaga: SCIENCE Vol. **286** (8 October 1999) 261.
[2] W. Fujita, K. Awaga, H. Matsuzaki and H. Okamoto, Phys. Rev. B 65, 064434 (2002)
[3] J. Takeda, M. Imae, S. Kurita and T. Kodaira: preprint (PIPT2001).
[4] G. Kresse and J. Furthmüller, Comput. Mater. Sci. **6**, 15 (1996); Phys. Rev. B **54**, 11 169 (1996).
[5] K. Ohno, Y. Maruyama, K. Esfarjani, Y, Kawazoe, N. Sato, R. Hatakeyama, T. Hirata, and M. Niwano, Phys. Rev. Lett. **76**, 3590 (1996).
[6] K. Ohno, F. Marui and S. G. Louie, Phys. Rev. B **56**, 1009 (1997).
[7] S. Ishii, K. Ohno and Y. Kawazoe, Mater. Trans. JIM **40**, 1209 (1999).
[8] D. M. Ceperley and B. J. Alder, Phys. Rev. Lett. **45**, 566 (1980).
[9] J. P. Ferraris, D. O. Cowan, V. Walatha, Jr., and J. H. Perlstein, J. Am. Chem. Soc. **95**, 948 (1973).
[10] S. L. Adler, Phys. Rev. **126**, 413 (1962).

(Received December 20, 2002; Accepted March 1, 2003)